

# Graft Copolymerization of Soybean Protein Isolate and Methacrylic Acid

Cheng Yang, Xiaoqing Song, Chao Sun, Mingqing Chen, Yulan Xu, Xiaoya Liu, Zhongbin Ni

School of Chemical and Material Engineering, Southern Yangtze University, Wuxi, Jiangsu 214036, People's Republic of China

Received 31 August 2005; accepted 26 December 2005

DOI 10.1002/app.23993

Published online in Wiley InterScience (www.interscience.wiley.com).

**ABSTRACT:** Graft copolymers of soybean protein isolate (SPI) and methacrylic acid (MAA) were prepared in an 8 mol/L urea aqueous solution with ammonium persulfate (APS) as an initiator,  $\beta$ -mercaptoethanol as an unfolding agent for SPI, and a chain-transfer agent. Evidence of grafting was obtained by the comparison of the Fourier transform infrared and NMR spectra of SPI with those of the SPI-grafted MAA copolymer [SPI-g-poly(methacrylic acid) (PMAA)]. A possible copolymerization mechanism of SPI and MAA was determined, and the copolymerization rate equation was derived. The effect of  $\beta$ -mercaptoethanol content, APS content, and reaction temperature on the graft copolymerization was studied by the determination of the

grafting parameters, including grafting percentage and grafting efficiency. Dynamic laser light scattering was used to investigate the effect of the pH value on the hydrodynamic radius of SPI and the grafted SPI aggregate in aqueous solution. The average hydrodynamic radius of SPI-g-PMAA aggregate was much smaller than that of the SPI aggregate at about the isoelectric point of SPI and a high pH value, and the hydrodynamic radius distribution of the SPI-g-PMAA aggregate was narrower than that of the SPI aggregate. © 2006 Wiley Periodicals, Inc. *J Appl Polym Sci* 102: 4023–4029, 2006

**Key words:** biodegradable; graft copolymers; light scattering; proteins; synthesis

## INTRODUCTION

Soybean protein isolate (SPI) is the main component of the soybean, which is primarily an industrial crop cultivated for oil and protein. Other components of the soybean are fat, cellulose, impurities, and so on. The protein content of SPI is above 90%. SPI has a high soluble protein content and excellent functional properties, including solubility, gelation, elasticity, emulsification, and foaming.<sup>1</sup> More and more methods have been used to modify SPI to improve its functional properties by the alteration of its molecular structure or conformation.<sup>2–4</sup> The methods normally used to denature proteins include the cleavage of proteins,<sup>5–7</sup> crosslinking,<sup>8</sup> enzyme modification,<sup>9–11</sup> chemical modification,<sup>12–14</sup> and interaction with polysaccharides.<sup>15</sup> Recently, due to their degradable properties, protein-based materials have attracted much interest. However, the strength of materials made of pure SPI are so low that they hardly have application value. So, the modification of SPI by grafting copolymerization with other functional monomers and the blending of SPI with other synthesized polymers have been important for protein-

based materials.<sup>16–19</sup> However, in our knowledge, only a few investigations have referred to the graft copolymerization of SPI.<sup>16–19</sup> The solubility of SPI in dilute aqueous solution without a denatured agent was about 65 g/100 g of protein and decreased to 20 g/100 g of protein with increasing concentration up to 20% (w/w).<sup>20</sup> The low solubility of SPI in aqueous solution would adversely influence the quality of protein-based materials manufactured by the solution casting method. Poly(methacrylic acid) (PMAA) is a typical polyelectrolyte, and the grafting of methacrylic acid (MAA) on the SPI would change the physicochemical properties of SPI in aqueous solution. It would be helpful to widen the application of SPI or improve the properties of SPI-based materials.

In this study, we investigated the graft copolymerization of MAA onto SPI in an 8 mol/L urea aqueous solution with  $\beta$ -mercaptoethanol as an unfolding agent for SPI, a chain-transfer agent, and ammonium persulfate (APS) as an initiator. The mechanism of the grafting of MAA on SPI is discussed in detail. The effect of pH on the SPI-g-PMAA aggregates in aqueous solution was also investigated by dynamic laser light scattering.

Correspondence to: X. Liu (lxy@sytu.edu.cn).

Contract grant sponsor: National Natural Science Foundation of China; contract grant numbers: 20374025, 20476040, 20506008.

## EXPERIMENTAL

### Materials

SPI was supplied by the Sanjiang Co. (Heilongjiang, China). The content of protein was determined by

an automatic flash combustion method with a nitrogen analyzer NA2000 (CE Instruments, Italy). A conversion factor of 6.25 was used to calculate the protein content. The content of protein was 90%. The remaining 10% of the SPI was moisture (6%), impurities (3%), fat (0.5%), and fiber (0.5%). APS and  $\beta$ -mercaptoethanol were analytical grade and were used as purchased from Sigma Co. (St Louis, MO). MAA was purchased from Shanghai Chemical Co. (Shanghai, China) and was distilled under reduced pressure at 75°C. It was stored at -10°C until it was used.

### Graft copolymerization

A 100-mL three-necked round-bottom flask fitted with a stirrer in a temperature-controlled water bath was used for the reaction. A typical grafting reaction was carried out as follows: 1 g of SPI was dispersed in 50 mL of 8 mol/L urea solution with stirring under a nitrogen atmosphere at  $60 \pm 2^\circ\text{C}$  for about 30 min. Then, 2 mL of  $\beta$ -mercaptoethanol was added to the flask to cleave the disulfide bonds of SPI for 1 h. This treatment was followed by the addition of 0.17 g of APS and 2 g of MAA. After it proceeded at  $60 \pm 2^\circ\text{C}$  for 2 h, we stopped the reaction by cooling the flask and pouring the reaction mixture into 250 mL of acetone. The precipitate was collected by centrifugation at 8000 rpm for 30 min and was then extracted in a Soxhlet apparatus by refluxing in alcohol for 36 h to remove the PMAA homopolymer and the unreacted monomer. Finally, the copolymer was dried in a vacuum oven at  $30 \pm 5^\circ\text{C}$  to a constant weight. A parallel experiment was carried out by the same method as described except without the addition of the MAA monomer and APS initiator. The grafting percentage (GP) and grafting efficiency (GE) were calculated from the following relations:<sup>21</sup>

$$\text{GP (\%)} = \frac{W_1 - W_0}{W_0} \times 100 \quad (1)$$

$$\text{GE (\%)} = \frac{W_1 - W_0}{W_2} \times 100 \quad (2)$$

where  $W_0$ ,  $W_1$ , and  $W_2$  denote the weights of the SPI, graft copolymer, and monomer, respectively.

The overall copolymerization rate ( $R_p$ ) were calculated as follows:

$$R_p = \frac{W_1 - W_0}{t \times m \times V} (\text{mol L}^{-1}\text{s}^{-1}) \quad (3)$$

where  $W_0$  and  $W_1$  are the weights of the SPI and graft copolymer, respectively, and  $t$ ,  $m$ , and  $V$  are the reaction time, MAA monomer molecular weight, and reaction volume, respectively.

### Fourier transform infrared (FTIR) study

The FTIR spectra of grafted SPI, SPI and PMAA, and the parallel reaction production were run in the form of KBr pellets on FTLA2000-104 spectrophotometer (ABB Co., Canada) in the frequency range 4000–500  $\text{cm}^{-1}$ .

### <sup>13</sup>C-NMR study

The solid-state <sup>13</sup>C-NMR spectroscopy of grafted SPI and SPI was carried out on a JNM-MY60FT spectrometer (Jeol Co., Japan) with a frequency of 75 MHz at room temperature. The contact time for the cross-polarization process was 2.0 ms. The pulse width was 4.1  $\mu\text{s}$ , the magic-angle spinning rate was set to 3 kHz, and the repetition time was 5 s. The <sup>13</sup>C chemical shift of the carbonyl carbon signal of glycine (176.03 ppm relative to tetramethylsilane) was used as an external reference standard.

### Determination of the SH groups

SH groups were determined with the use of 5,5'-dithiobis(2-nitrobenzoic acid) according to Shimada and Cheftel<sup>20</sup> and Ellman.<sup>22</sup> To a 3-mL aliquot of standard buffer solution (10 g/mL, pH 8.0) of the native SPI or parallel reaction product was added 0.03 mL of Ellman's reagent solution [4 mg of 5,5'-dithiobis(2-nitrobenzoic acid)/mL of standard buffer]. After the solution was rapidly mixed and allowed to stand at room temperature for 15 min, the absorbance was read at 412 nm. The standard buffer was used as a reagent blank. A molar extinction coefficient of 13,600  $\text{M}^{-1}\text{cm}^{-1}$  was used to calculate the micromoles of SH per gram of SPI and parallel reaction product.

### Dynamic laser light scattering

A modified commercial laser light scattering spectrometer (ALV/DLS/SLS-5022F, ALV Co., Germany) was used; it was equipped with an ALV-5000 multi- $\tau$  digital time correlator and a He-Ne laser (uniphase, output power  $\approx 20$  mW at  $\lambda = 632.8$  nm). In dynamic LLS, the intensity-intensity time correlation function [ $G^2(t, q)$ ] in the self-beating mode was measured, where  $t$  is the delay time. For broadly distributed relaxation, the characteristic relaxation (decay) time distribution [ $G(\tau)$ ] can be calculated from the Laplace inversion of the measured  $G^2(t, q)$ . For a pure diffusive relaxation,  $(\Gamma/q^2)_{q \rightarrow 0, c \rightarrow 0}$  leads to the translational diffusion coefficient ( $D$ ), which is further related to the hydrodynamic radius ( $R_h$ ) by the Stokes-Einstein equation:  $R_h = k_B T / (6\pi\eta D)$ , where  $k_B$ ,  $T$ , and  $\eta$  are the Boltzmann constant, absolute temperature, and solvent viscosity, respectively.

The grafted SPI and SPI in aqueous solution with different pH values were prepared for the light scattering experiment. The different pH values of the aqueous solution were adjusted by the addition of

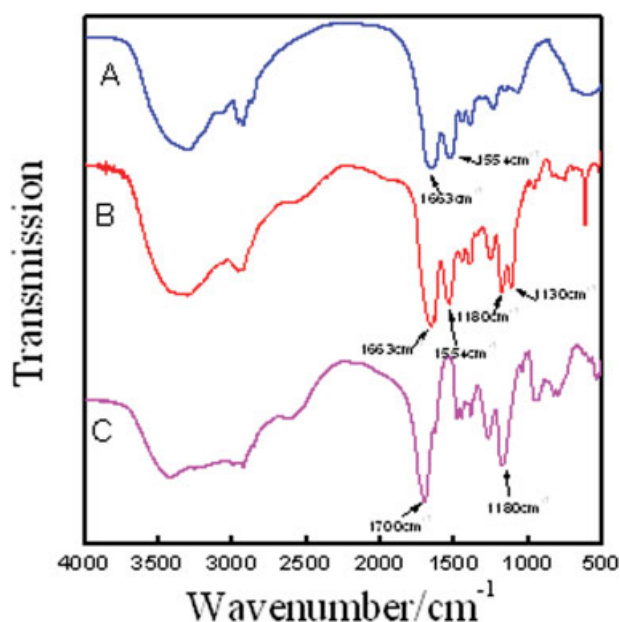


**Figure 1** FTIR spectra of (A) SPI, (B) SPI-g-PMAA (GP = 114%) and (C) PMAA homopolymer. [Color figure can be viewed in the online issue, which is available at [www.interscience.wiley.com](http://www.interscience.wiley.com).]

6M NaOH or 6M HCl solution, and at the same time, 6M NaCl solution was added to preserve a constant ionic strength. The solutions were passed through a 1- $\mu\text{m}$  or 0.45- $\mu\text{m}$  Millipore filter into a dust-free cell for the light scattering experiment. The laser light scattering experiments were carried out at a scattering angle of  $90^\circ$  and at  $25 \pm 0.1^\circ\text{C}$ .

## RESULTS AND DISCUSSION

### FTIR study of SPI-g-PMAA

The FTIR spectra of the SPI, SPI-g-PMAA, and the PMAA homopolymer are shown in Figure 1. The most important absorption peaks for PMAA were at 1700 and  $1180\text{ cm}^{-1}$ . These peaks were caused by C=O stretching vibrations and C—O stretching vibrations, respectively. The well-characterized absorption peaks for SPI were at 1663 and  $1545\text{ cm}^{-1}$ . They were caused by the carboxyl and amide groups of SPI, respectively. This was in agreement with the experimental results of Wu and Zhang.<sup>23</sup> Compared with the spectra of PMAA, SPI, and the graft SPI, the observed absorption peaks at 1663 and  $1180\text{ cm}^{-1}$  for the graft copolymer indicated that the MAA had grafted onto SPI.

### NMR study of SPI-g-PMAA

The  $^{13}\text{C}$ -NMR spectra of the SPI-g-PMAA and SPI are shown in Figure 2. SPI contains many kinds of amino acids. Glutamic acid, aspartic acid, arginine, and lysine are the main kinds of amino acid in SPI.

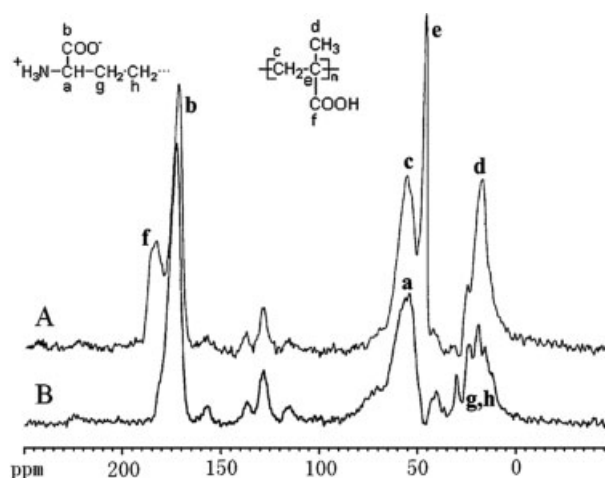


**Figure 2**  $^{13}\text{C}$ -NMR spectra of (A) SPI-g-PMAA (GP = 114%) and (B) SPI.

Their normal chemical formula is shown in Figure 2. Peak (a) at  $\delta = 54\text{ ppm}$  and peak (b) at  $\delta = 173\text{ ppm}$  appeared in the spectra of both ungrafted SPI and SPI-g-PMAA and were attributed to the carbon atom of CH groups ( $\alpha\text{ C}$  atom) and COO groups of the amino acids of SPI, respectively. The peaks (g, h, . .) at  $\delta = 16\text{--}40\text{ ppm}$  could be attributed to the  $\beta, \gamma, \dots\text{C}$  atom of amino acid of SPI. Peak (c) at  $\delta = 55\text{ ppm}$ , peak (d) at  $\delta = 16\text{ ppm}$ , peak (e) at  $\delta = 46\text{ ppm}$ , and peak (f) at  $\delta = 184\text{ ppm}$ , all of which appeared in the spectra of SPI-g-PMAA, could be attributed to the carbon atoms of  $\text{CH}_2$ ,  $\text{CH}_3$ , C, and COOH of MMA, respectively. This was in agreement with the  $^{13}\text{C}$ -NMR spectra of PMAA reported by Chen et al.<sup>24</sup> and Yi and Goh.<sup>25</sup> Therefore, the graft copolymerization of MAA onto SPI was further proved by the NMR spectrum.

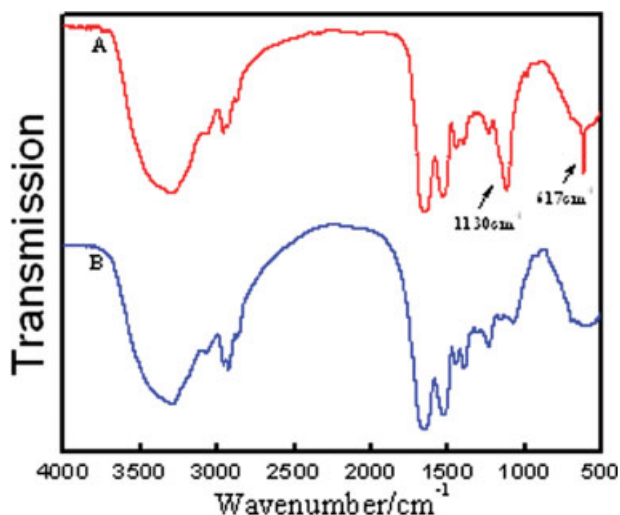


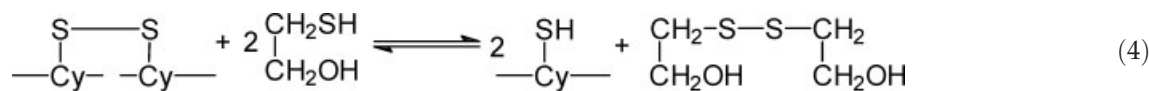
**Figure 3** FTIR spectra of (A) parallel experiment product and (B) SPI. [Color figure can be viewed in the online issue, which is available at [www.interscience.wiley.com](http://www.interscience.wiley.com).]

### Copolymerization mechanism

Although the copolymerization of SPI and MAA was carried out with APS as the initiator and without the addition of  $\beta$ -mercaptoethanol, no MAA adsorption peaks were found in the FTIR spectra of the reaction product and  $GP = 0$ . This indicated that without  $\beta$ -mercaptoethanol, APS could not initiate the copolymerization of SPI and MAA. To understand the effect of  $\beta$ -mercaptoethanol on SPI, a parallel experiment was carried out that was the same as the copolymerization of SPI and MAA except without the addition of the APS initiator and MAA monomer. The FTIR spectra of the parallel reaction product after the removal of  $\beta$ -mercaptoethanol and the spectra of SPI are shown in Figure 3. Figure 3 shows that compared with the spectra of SPI, the spectra of the parallel reaction product had strong absorption peaks at 1130 and 617  $\text{cm}^{-1}$ , which were attributed to the  $-\text{C}-\text{O}$  stretching vibrations and  $-\text{C}-\text{S}$  stretching vibrations, respectively. This suggests that  $\beta$ -mercaptoethanol cleaved the di-

sulfide bonds of SPI and made the SPI unfold and thus exposed more carboxyl and sulfhydryl groups of SPI. Furthermore, the SH group contents of native SPI and the parallel reaction product were determined by the Ellman<sup>22</sup> method. The content of SH groups was 3.5  $\mu\text{mol/g}$  for native SPI and 30.8  $\mu\text{mol/g}$  for the parallel reaction product, respectively. This also indicated that the disulfide bond of SPI was cleaved by  $\beta$ -mercaptoethanol. The average number of disulfide bonds in a SPI molecule is about 23, and they exist in the cystine (Cy) unit of SPI.<sup>26</sup> Many  $-\text{C}-\text{SH}$  groups would be produced if all the disulfide bonds were cleaved. These groups were easily attacked by the APS initiator and formed the radicals to initiate the graft copolymerization between the SPI and MAA. Therefore, the mechanism of the grafting of MAA onto SPI with  $\beta$ -mercaptoethanol as an unfolding agent for SPI might be proposed as follows:

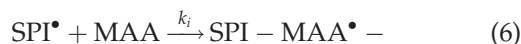
Cleavage of disulfide bonds and SPI unfolding



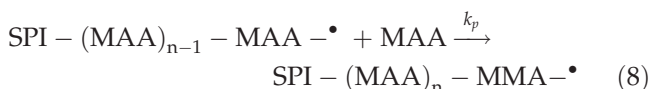
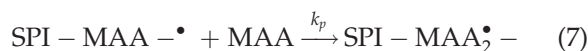
Radical formation



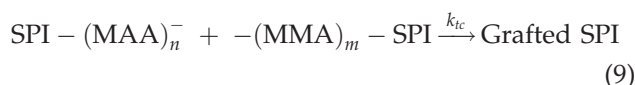
Initiation



Propagation



Termination



If one considers that eqs. (5) – (9) were the copolymerization of SPI and MAA,  $R_p$  could be derived from the following equation:

$$R_p = k_p(k_d/k_{tc})[\text{SPI}]^{1/2}[\text{APS}]^{1/2}[\text{MAA}] \quad (10)$$

where  $k_d$  is the radical formation rate constant and  $k_i$ ,  $k_p$ , and  $k_{tc}$  are the initiation, propagation, and ter-

mination rate constants, respectively, for the copolymerization of SPI and MAA. If the proposed copolymerization mechanism was right, according to the eq. (10), the plots of  $R_p$  versus  $[\text{APS}]^{1/2}$  and  $R_p$  versus  $[\text{MAA}]$  would be lines. The experimental results (shown in Figs. 4 and 5) indeed show that plots of  $R_p$  versus  $[\text{APS}]^{1/2}$  and  $R_p$  versus  $[\text{MAA}]$  were lines when  $[\text{APS}]$  was lower than 16 mmol/L. This indicated that the supposed copolymerization steps were right. When  $[\text{APS}]$  was higher than 16 mmol/L,  $R_p$  was not in proportion to  $[\text{APS}]^{1/2}$ . This could be

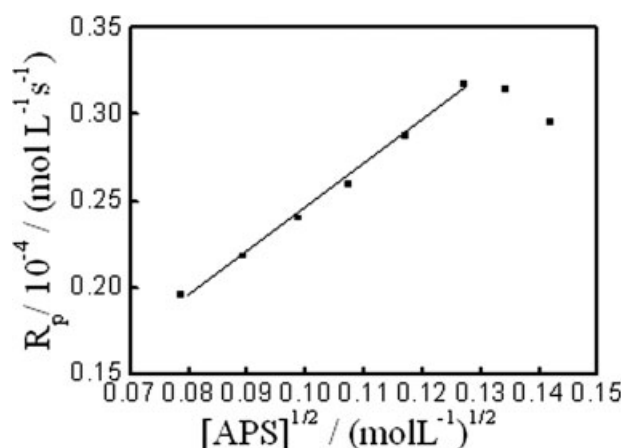


**Figure 4** Plot of  $R_p$  versus  $[\text{APS}]^{1/2}$ :  $[\text{SPI}] = 20 \text{ g/L}$ ,  $[\text{MAA}] = 0.46 \text{ mol/L}$ , and temperature =  $60^\circ\text{C}$ .

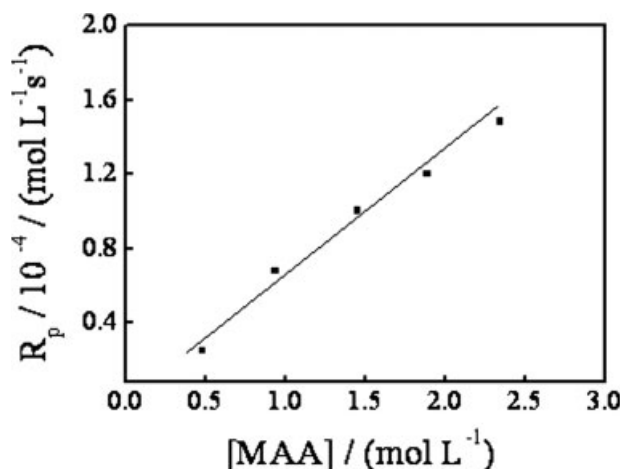


**Figure 5** Plot of  $R_p$  versus [MAA]: [SPI] = 20 g/L, [APS] = 14 mmol/L, and temperature = 60°C.

explained by the enhancement of the MAA homopolymerization and chain-transfer reaction with the increase of [APS].

#### Effect of the $\beta$ -mercaptoethanol concentration on GP and GE

Figure 6 shows that GP and GE increased from 75 and 38% to 120 and 61%, respectively, with the increase of  $\beta$ -mercaptoethanol content from 0.028 mol/L up to 0.1 mol/L. This was reasonable because more disulfide bonds of SPI would have been cleaved with increasing  $\beta$ -mercaptoethanol content, resulting in the rise of the reactivity of SPI. However, when the  $\beta$ -mercaptoethanol content was beyond 0.1 mol/L, GP and GE decreased to 35 and 18%, respectively, with increasing  $\beta$ -mercaptoethanol content up to 0.54 mol/L. It is well known that  $\beta$ -mercaptoethanol is a chain-transfer agent for radical polymerization so that the chain-

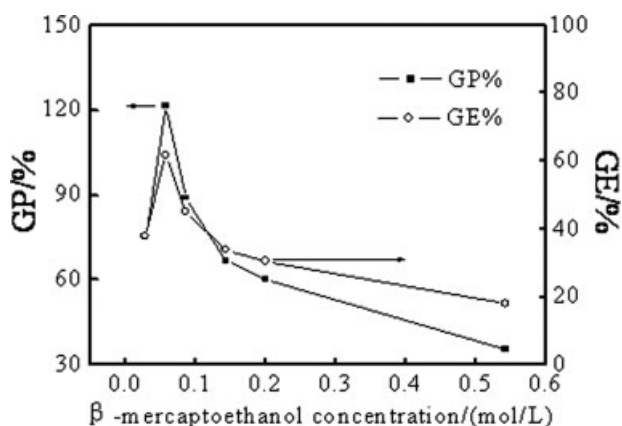


**Figure 6** Effect of  $\beta$ -mercaptoethanol on GP and GE: [SPI] = 20 g/L, [MAA] = 0.46 mol/L, [APS] = 14 mmol/L, and temperature = 60°C.

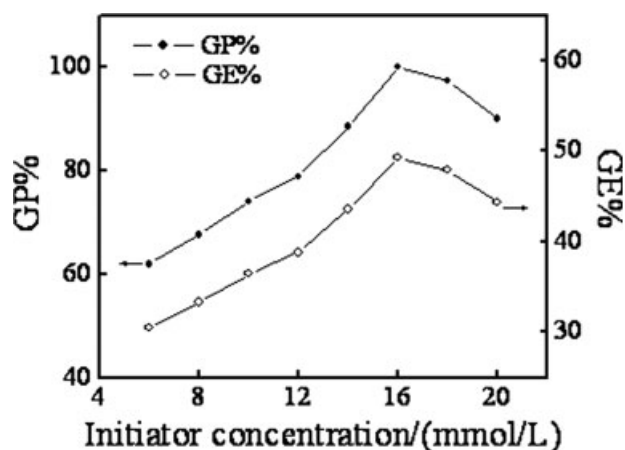


**Figure 7** Effect of initiator concentration on GP and GE: [SPI] = 20 g/L, [MAA] = 0.46 mol/L, reaction time = 120 min, and temperature = 60°C.

transfer reaction increases with increasing  $\beta$ -mercaptoethanol concentration. Thus, GP and GE would decrease with increasing  $\beta$ -mercaptoethanol concentration when it goes beyond a maximum value.

#### Effect of the initiator concentration on GP and GE

As shown in Figure 7, with increasing initiator concentration, GP and GE increased steadily from 62 and 30% to 49 and 100%, respectively, and then decreased after an optimum value of 16 mmol/L. The initial rise in GE and GP could be attributed to the increase in macroradicals. As the concentration of APS increased, more APS attacked the mercaptoes of SPI and more SPI macroradicals formed in the SPI main chain to initiate grafting copolymerization, which caused the GP and GE to increase. However, when the concentration of APS was higher than 16 mmol/L, abundant free radicals and macroradicals formed, and they could terminate the growing chain or initiate the homopolymerization of MAA. This resulted in a decrease of GP and GE.

#### Effect of temperature on the copolymerization

The effect of temperature on the graft copolymerization was investigated over the range 40–100°C, and the results are shown in Figure 8. GP and GE increased to their maximum value (148 and 73%, respectively) at about the rate of 3%/°C with increasing temperature up to 80°C, and beyond this maximum, they decreased at about a rate of 4%/°C with increasing temperature. At low temperatures, the redox reaction between APS and SPI was slow, as was the formed radical content. In that case, GP and GE were also low. With increasing temperature, the redox reaction became easier, and the macroradical content increased so that the graft copolymerization was enhanced. This led to the

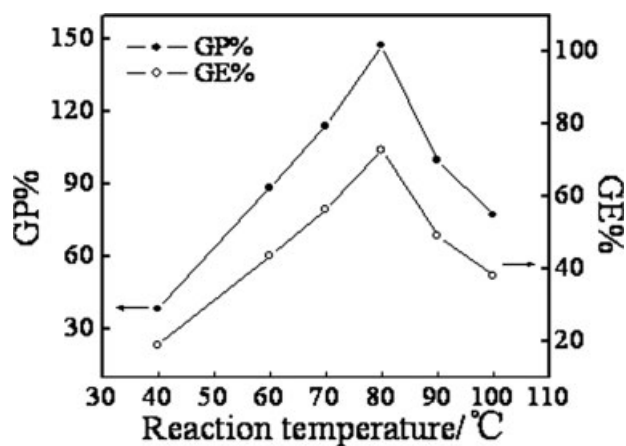


**Figure 8** Effect of reaction temperature on GP and GE: [SPI] = 20 g/L, [MAA] = 0.46 mol/L, [APS] = 14 mmol/L, and reaction time = 120 min.

increase in GE and GP. However, when the temperature was higher than 80°C, the termination reaction between the radicals and the homopolymerization of monomer MAA were enhanced, with the result that GE and GP decreased.

#### Effect of pH value on the aggregation of SPI and SPI-g-PMAA

Currently, protein-based materials are mainly manufactured by the solution casting method. Thus, the investigation of the solution properties of SPI and SPI-g-PMAA is important for their application. SPI can aggregate in an aqueous solution induced by pH value, heat, or high concentration. The size and structure of the SPI aggregates will be related to the properties of SPI-based food, plastic, fiber, and so on. In this study, during the extracting process, the SPI, induced by heat, aggregated and could not redisperse as single molecules in aqueous solution so that the effect of temperature on the aggregated SPI was insignificant. However, SPI is composed of charged amide groups and acid groups. Thus, the pH value of solution will influence the conformation and aggregation of SPI. Figure 9 shows that average hydrodynamic radius ( $\langle R_h \rangle$ ) of SPI increased sharply up to 800 nm at a pH of about 4.5. Because the isoelectric point of pure SPI is about pH 4.5,<sup>27</sup> the charge of SPI at this pH value is zero. Such being the case, SPI became hydrophobic and settled into huge aggregates and might deposit from the solution. When the pH value of solution deviated from the isoelectric point of SPI, the SPI aggregate with  $\langle R_h \rangle$  of about 100 nm could steadily disperse in the aqueous solution.  $\langle R_h \rangle$  of SPI increased from 72 to 141 nm with increasing pH value from 7.5 to 12. When the pH value grew beyond 12,  $\langle R_h \rangle$  of the SPI aggregate increased sharply to 580 nm. We could not account for why the  $\langle R_h \rangle$  of SPI and SPI-g-PMAA increased so much when

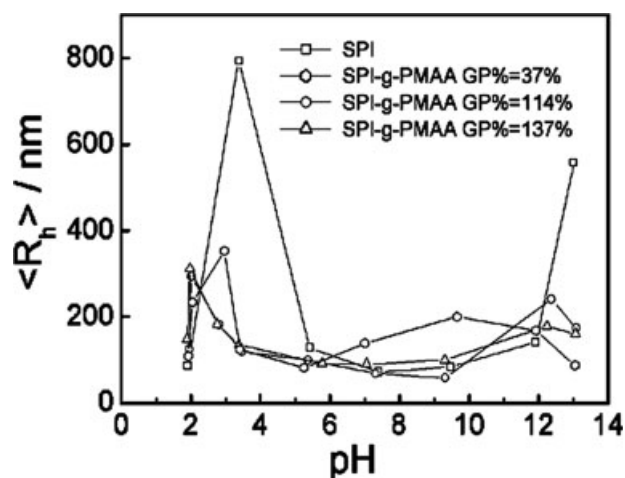


**Figure 9** Effect of pH value on  $\langle R_h \rangle$  of the SPI aggregate and SPI-g-PMAA aggregate in aqueous solution.

the pH value was beyond 12. Figure 9 also shows that  $\langle R_h \rangle$  of the SPI-g-PMAA aggregate were about 300 and 170 nm at the isoelectric point of SPI and a high pH value (13), respectively, which were much smaller than that of SPI. With increasing GP,  $\langle R_h \rangle$  of SPI-g-PMAA decreased at the isoelectric point of SPI and high pH value (13). This indicated that grafting of MAA onto the SPI changed the charge density of SPI and increased the hydrophilicity of the SPI. Although  $\langle R_h \rangle$  of SPI-g-PMAA was nearly the same as that of SPI when the pH value deviated from the isoelectric point of SPI,  $\langle R_h \rangle$  of SPI-g-PMAA was narrower than that of SPI (shown in Fig. 10). In contrast with the polydispersity of the SPI aggregate dispersion, the narrowly distributed SPI-g-PMAA aggregate, when cast from the solution, formed SPI-based material with a more homogeneous microstructure. This would be more favor-

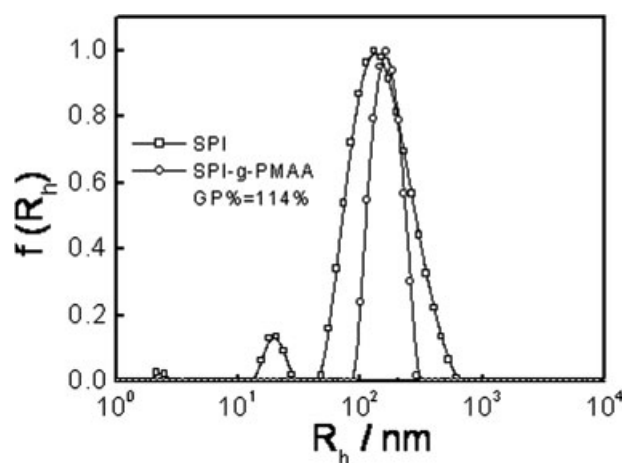


**Figure 10**  $R_h$  distribution of the SPI aggregate and SPI-g-PMAA aggregate in aqueous solution (pH = 8.5).

able to the physical properties of SPI-based materials, such as films and fibers.

### CONCLUSIONS

MAA was successfully grafted onto SPI with  $\beta$ -mercaptoethanol as an unfolding agent for SPI, a chain-transfer agent, and APS as an initiator.  $R_p$  was in proportion to  $[\text{APS}]^{1/2}$  and  $[\text{MAA}]$ . GP and GE increased with increasing initiator concentration primarily and then decreased after an optimum value of 16 mmol/L was reached. GP and GE increased with increasing temperature up to 80°C, and beyond this maximum, they decreased with increasing temperature.  $\langle R_h \rangle$  of the SPI-g-PMMA aggregate was much smaller than that of the SPI aggregate at about the isoelectric point of SPI and high pH value, and the  $R_h$  distribution of the SPI-g-PMMA aggregate was narrower than that of the SPI aggregate.

### References

1. John, E. K. *J Am Oil Chem Soc* 1979, 56, 242.
2. Kumar, R.; Choudhary, V.; Mishra, S.; Varma, I. K.; Mattiason, B. *Ind Crops Prod* 2002, 16, 155
3. Feeney, R. E.; Whitaker, J. R. *Food Proteins: Improvement Through Chemical and Enzymatic Modification*; Advances in Chemistry Series 160; American Chemical Society: Washington, DC, 1977; p 3.
4. Feeney, R. E.; Whitaker, J. R. In *Chemical and Enzymatic Modification of Plant Proteins in New Protein Foods*; Altschul, A. M.; Wilcke, H. L., Eds.; Academic: New York, 1985; p 181.
5. Nir, I. Y.; Feldman, Y.; Aserin, A. *J. Food Sci* 1994, 59, 606.
6. Rhim, J. W.; Gemmadios, A.; Weller, C. L.; Hanna, M. A. *Ind Crops Prod* 2002, 15, 199.
7. Molina, M. I.; Wagner, J. R. *Food Res Int* 1999, 32, 135.
8. Park, S. K.; Bae, D. H.; Rhee, K. C. *J Am Oil Chem Soc* 2000, 77, 879.
9. Sara, E. M. O.; Maria, C. A. *J Am Oil Chem Soc* 2000, 77, 1293.
10. Ruth, L. N.; Flavia, M. N. *J. Agric Food Chem* 1998, 46, 3009.
11. Calderon, D. B. A. M.; Ruiz-Salazar, R. A.; Jara-Marini, M. E. *J Food Sci* 2000, 65, 246.
12. Kalapathy, U.; Hettiarachchy, N. S.; Rhee, K. C. *J Am Oil Chem Soc* 1997, 74, 195.
13. Barman, B. G. *J. Agric Food Chem* 1997, 25, 618.
14. Kim, S. H.; Kinsella, J. E. *J. Food Sci* 1987, 52, 128.
15. Cabodevila, O. *J. Food Sci* 1994, 59, 872.
16. Lu, B. K.; Guo, S. J.; Gao, Z. X.; Guo, Y. L. *Chin. Pat. CN* 1308151A (2001).
17. Steinmetz, A. L.; Krinski, T. L. *U.S. Pat.* 4,687,826 (1987).
18. Steinmetz, A. L.; Krinski, T. L. *U.S. Pat.* 4,554,337 (1985).
19. Dykstra, G. M.; Hollingsworth, R. L. *U.S. Pat.* 3,920,592 (1975).
20. Shimada, K.; Cheftel, J. C. *J. Agric Food Chem* 1988, 36, 147.
21. Athawale, V. D.; Lele, V. *Carbohydr Polym* 1999, 41, 407.
22. Ellman, G. L. *Arch Biochem Biophys* 1959, 82, 70.
23. Wu, Q.; Zhang, L. *J Appl Polym Sci* 2001, 82, 3373.
24. Zhao, H.; Lin, W.; Yang, G.; Chen, Q. *Eur Polym J* 2005, 41, 2354.
25. Yi, J. Z.; Goh, S. H. *Polymer* 2001, 42, 9313.
26. Bigelow, C. *Theorem Boil* 1967, 16, 187.
27. Smith, A. K.; Circle, S. J. *Soybean: Chemistry and Technology*; AVI: Westport, CT, 1978.